An identification scheme of grain boundaries and construction of a grain boundary energy database

Hyun-Kyu Kim,[a] Won-Seok Ko,[a] Hyuk-Joong Lee,[a] Seong Gyoon Kim[b] and Byeong-Joo Lee[a,*,1]

[a]Department of Materials Science and Engineering, Pohang University of Science and Technology (POSTECH), Pohang 790-784, Republic of Korea
[b]Department of Materials Science and Engineering, Kunsan National University, Kunsan 573-701, Republic of Korea

We have developed a systematic scheme to identify and distinguish individual grain boundaries from one another according to the misorientation and inclination in polycrystalline materials. This allows us to construct a grain boundary energy database in a suitable form for implementation on mesoscale grain growth simulations. The scheme can be equally applied to identify interfaces between two different phase grains, and enables realistic simulations of phase transformations as well as grain growth, assigning real crystallographic orientations to individual grains.
© 2011 Acta Materialia Inc. Published by Elsevier Ltd. All rights reserved.

Microstructures evolve during phase transformations, recrystallizations and grain growth in bulk or thin film polycrystalline materials. In addition to the relationship of grain size distribution and morphology to texture and abnormal grain growth, the microstructural evolution has a decisive effect on the structural and functional properties of materials. Due to the crucial role of microstructures on the properties of materials, many simulation studies have been carried out to predict, understand and control microstructural evolution.

Since microstructural evolution is known to be highly dependent on the anisotropy of grain boundary properties such as grain boundary energy and mobility, a great deal of effort has also been focused on calculating the energy and mobility of grain boundaries with various misorientation relationships [1–22]. However, these calculations have mostly been performed only for specially selected grain boundaries, i.e. symmetric tilt, twist or coincident site lattice (CSL) boundaries, in a functional form with one degree of freedom, i.e. the misorientation or the Σ value. It has proved impossible to perform grain growth simulations that assign specific crystallographic orientations to individual grains and consider the anisotropic properties of all possible grain boundaries.

One should note here that there can be an infinite number of different grain boundaries depending on the orientation relationship between the two grains that form the grain boundary. A grain boundary between two crystalline solids is uniquely defined in a three-dimensional space when five macroscopic degrees of freedom are fixed [23,24]: three are from the orientation difference between the two crystals, and two are from the inclination of the boundary. Therefore, grain boundary properties should be provided as a function of the above-mentioned five degrees of freedom in order to be able to be used in grain growth simulations.

Such an expression of the grain boundary properties was provided by Rohrer and coworkers [25–30] who discretized the misorientation and inclination angles and presented the distribution and relative energies of grain boundaries as a function of the five degrees of freedom. Even with this progress, grain growth simulations based on realistic crystallographic orientations of individual grains and realistic grain boundary properties (e.g. grain boundary energy) have not been performed. This may be due to the fact that the calculation of grain boundary energy for a wide range of different grain boundaries is not trivial.

Inspired by the pioneering work by Rohrer and coworkers [25–30], we provide here a systematic scheme

* Corresponding author. Tel.: +82 54 2792157; fax: +82 54 2792399; e-mail: calphad@postech.ac.kr
1 Presently on leave at Computational Science Center, KIST, Republic of Korea.

to uniquely identify individual grain boundaries among all possible grain boundaries in polycrystalline materials. The scheme is applied to a representative material with a cubic crystallographic symmetry, iron. Based on the scheme, a grain boundary energy database is constructed for body-centered cubic (bcc) Fe using an atomistic approach (molecular statics), in a suitable form for implementation on grain growth simulations. The grain boundary energies are calculated for systematically selected grain boundaries on the basis of the five degrees of freedom. The three translational degrees of freedom at the boundary [24] are thought to be automatically minimized during the atomistic calculation, just as they are in reality [1].

Before going into details of the scheme, the way of representing the orientation relationship between a polycrystalline specimen and individual grains should be explained. The coordinate system of the specimen, K_s, is defined using three axes, x_1, x_2 and x_3, for example, along the rolling (RD), transverse (TD) and normal (ND) directions, respectively. The coordinate system of a specific grain, K_c, can be represented by rotating the coordinate system of the specimen in an axial (passive) transformation:

$$K_c = g \cdot K_s \qquad (1)$$

The rotation matrix g is a 3×3 tensor. The rotation can be performed by using three Euler angles, (ϕ_1, Φ, ϕ_2) [31], where ϕ_1 is an angle of rotation around ND, Φ around the new RD and ϕ_2 around the new ND. The overall rotation tensor g is obtained by $g = g_{\phi_1} \cdot g_\Phi \cdot g_{\phi_2}$. The crystallographic orientations of individual grains can be represented by the g tensors assigned to individual grains with respect to the coordinate system of the specimen. The misorientation between two neighboring grains can also be represented using the two g tensors assigned to the two grains. For example, if the rotation tensors for the two grains are g_{c1} and g_{c2}, then the misorientation between them is represented by $g_{c1}^{-1} \cdot g_{c2}$ (or $g_{c2}^{-1} \cdot g_{c1}$).

The first definition in the present scheme is the misorientation relationship between two neighboring grains. For this, consider a sphere inside a cube with the three [1 0 0] axes parallel to the x, y, z directions. Imagine that the two neighboring grains are rotated so that the crystallographic orientation of one grain corresponds to that of the cube and the orientation of the other grain to that of the sphere inside the cube. Figure 1 shows such a sphere inside a cube and shows that the misorientation between the sphere and cube can be represented by the above-mentioned rotation tensor operation. The rotation tensor, which describes the orientation of the sphere with respect to the cube and is represented by the three Euler angles (three degrees of freedom), uniquely defines the misorientation between the two neighboring grains. A tangent plane on the surface of the sphere (or radial direction from the center of the sphere to the tangent point), which is represented by two degrees of freedom (latitude and longitude or polar and azimuthal angles), uniquely defines the inclination between the two grains. Therefore, the grain boundary between two arbitrarily selected neighboring grains can be uniquely identified by defining the misorientation (the misorientation relationship between the sphere and the cube) and the inclination (a point on the surface of the sphere).
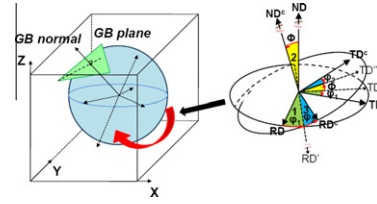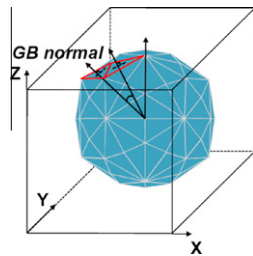

Figure 1. A scheme to identify the grain boundary between two neighboring grains. The misorientation between two grains is represented by the orientation of the sphere with respect to the coordinate system of the cube. A tangent plane on a surface point of the sphere corresponds to a grain boundary with an inclination represented by the radial direction to the tangent point.

A problem here is that both the misorientation and inclination angles are continuous quantities. There can be an infinite number of slightly different misorientation relations and also an infinite number of points on the surfaces. In order to be able to construct a practical grain boundary property database, one needs to discretize the misorientation and inclination angles. However, cubic crystal symmetry reduces the required range to $0 \leqslant \phi_1 \leqslant 90°$, $0 \leqslant \Phi \leqslant 90°$ and $0 \leqslant \phi_2 \leqslant 360°$, which nevertheless contains three copies of the fundamental zone. Combining two orientations together to compute a misorientation allows the range of Euler angles to be further reduced to $0 \leqslant \phi_1 \leqslant 90°$, $0 \leqslant \Phi \leqslant 90°$ and $0 \leqslant \phi_2 \leqslant 90°$, which nevertheless contains 48 copies of the fundamental zone [32]. In the present work, each Euler angle was divided into nine equal intervals (10 degrees) in the given range, which results in an identification of $9 \times 9 \times 9$ equally distributed different misorientations.

As already mentioned, the tangent plane on each point of the sphere shown in Figure 1 corresponds to a grain boundary plane with a specific inclination angle. Mesoscale simulations, such as the phase-field method, need information on the derivatives of grain boundary energy with respect to inclination angles to calculate the torques applied to a grain boundary, as well as the grain boundary energy itself. It would be easier to compute the derivatives if equally spaced points on the sphere are used. For this, the sphere inside the cube needs to be replaced by a polyhedron composed of identical polygons. In the present work, a disdyakis triacontahedron [33] covered with 120 triangular surface planes and 62 vertices was selected as shown in Figure 2. The total of 182 directions of the surface planes and vertices can be selected as the discretized inclination angles. However, since every two directions opposite to each other on the surface across the center of the sphere represent the same inclination, the surface planes and vertices on only a half sphere are enough to cover all probable inclination angles between two grains. It should be noted here that similar discretization of the five macroscopic parameter space has been done by Saylor et al. [27,29]. The only difference is that cosine values of some angles were discretized by Saylor et al., while the angles were discretized in the present study to make the computation of numerical derivatives easier.

The above discrete misorientation and inclination angles yield 66,339 ($9 \times 9 \times 9 \times 91$) evenly distributed grain boundaries for a cubic crystal. The resolution can be easily increased by reducing the size of the angular differences, if necessary. The second issue for the construction of a grain

Figure 2. A scheme to identify grain boundaries with discrete inclination angles, between two grains under a given misorientation.

boundary energy database is the computation of the grain boundary energy. An atomistic method (molecular statics) based on a second nearest-neighbor modified embedded-atom method (2NN MEAM) [34,35] interatomic potential was used for the computation.

Normally, the computation of grain boundary energy is done by comparing the energies of two samples, one with a grain boundary between two single crystals under a given misorientation and inclination, and the other without a grain boundary. The easiest way to make this comparison is to make the sample with the grain boundary have no other grain boundary or free surface, and compare the energy with the ideal bulk energy of a single crystal of the same material. The sample with only one type of grain boundary and no other grain boundary or free surface can be made by assigning a three-dimensional periodic boundary condition to the sample. However, it is generally impossible to assign a three-dimensional periodic boundary condition to a sample made by combining two crystals under an arbitrary misorientation and inclination. This is because the sample dimensions of each crystal in a direction parallel to the boundary where a periodic boundary condition is assigned are dissimilar.

A new method proposed [4] to overcome the abovementioned difficulty is to use a spherical sample as follows. Prepare two identical spherical samples and rotate each so that the two samples have a predetermined misorientation. Cut each spherical sample into two parts of exactly the same size, in a direction of a predetermined inclination angle. Then, combine the half spheres from each sample to make a new sphere that involves a newly created grain boundary under a given misorientation and inclination. Run a 0 K molecular statics allowing relaxation and compute the potential energy. The computed potential energy is different from that of the original sphere and the difference comes from the newly created grain boundary in the new sphere. An advantage of this method is that the procedure for computing the grain boundary energy for a series of different grain boundaries can be fully computerized because one does not need to adjust the sample size of each sample to apply the three-dimensional periodic boundary condition. This is the reason why the calculation for several tens of thousands of different grain boundaries can be performed within a practically reasonable time. It should be noted here that there can be a sphere size dependency in the computed grain boundary energy with this new method due to the intersection of the surface and boundary. This can be made negligible by using a sufficiently large sphere (diameter > 8 nm [4]).

The final issue with the present scheme and construction of the grain boundary energy database is that most of the special boundaries formed at a specific misorientation may not be identified using the current scheme based on the discrete misorientation and inclination angles. The special boundaries usually have a low energy compared to other high-angle boundaries and may have a significant effect on the microstructural evolution. Therefore, the using the grain boundary energy database to simulate the microstructure would be invalid if the special boundaries are not included in the database. This problem can be solved by constructing two separate databases, one for the ordinary grain boundary energy database based on the discrete misorientation and inclination angles, and the other for selected special boundaries. During the present work, it was found that CSL boundaries corresponding to $\Sigma \leqslant 33$ have a low energy and need to be considered. Eventually, 26 CSL boundaries [36] were selected and included in the special boundary database.

The calculated grain boundary energy of the 66,339 grain boundaries selected based on the discrete misorientation and inclination angles, and the energy of the 2366 (26×91) intentionally selected special boundaries, are illustrated in Figure 3a and b, respectively. Since the order of grain boundaries on the *x*-axis in Figure 3 has no special physical meaning, numerical values are also provided in a functional form for the five degrees of freedom (three Euler angles and two inclination angles) as supplementary online material of this paper. It is shown that the special boundaries have a stronger orientation dependency on the grain boundary energy compared to the other mechanically selected boundaries. As a means to further demonstrate the orientation dependency of grain boundary energy, we selected two special boundary sets, $\Sigma 3$ and $\Sigma 9$, and plotted the inclination dependency of boundary energy using color, as shown in Figure 4. Here, individual small spheres represent the surface planes and vertices on the disdyakis triacontahedron presented in Figure 2, and their color represents the size of the grain boundary energy. The axes *x*-*y*-*z* and *x'*-*y'*-*z'* represent the coordinate systems of cube and spherical grains, respectively. Miller indices of pure twist (or symmetric tilt) boundaries and the lowest and highest energy points are also presented. A strong anisotropy depending on the inclination is visible, and it turns out that pure twist (or symmetric tilt) boundaries correspond the lowest and highest energy boundaries. For example, Figure 4b shows that the (0 1 1) pure twist boundary is the lowest energy boundary among $\Sigma 9$ boundaries.
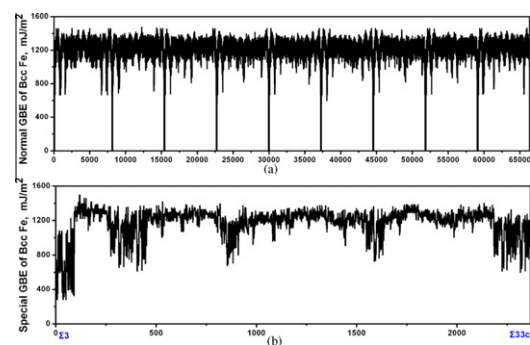
Figure 3. Calculated grain boundary energies of bcc Fe for (a) mechanically selected 66,339 grain boundaries and (b) intentionally selected 2366 special boundaries. Numerical values of misorientation/inclination angles and energy can be found in supplementary data files.
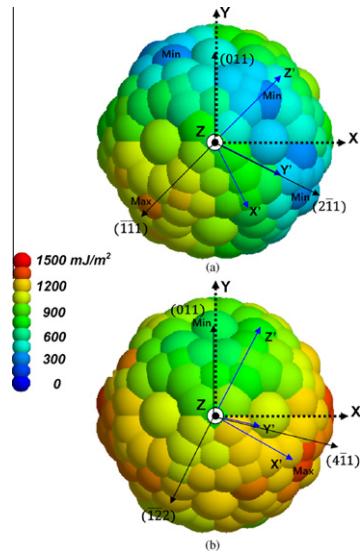
Figure 4. Anisotropy of grain boundary energy for (a) Σ3 and (b) Σ9 boundaries of bcc Fe depending on the inclination. Individual spheres represent the surface planes and vertices on the disdyakis triacontahedron presented in Figure 2, and their color represent the size of grain boundary energy (with "Max" and "Min" representing the highest and lowest energy). The axes *x-y-z* and *x'-y'-z'* represent the coordinate systems of cube and spherical grains, respectively. Miller indices of pure twist (or symmetric tilt) boundaries are also presented.

Table 1. Size of the Euler space necessary to uniquely represent misorientation for various crystal symmetries [36].

Crystal structure	Φ	ϕ_2	ϕ_1
Cubic	90°	90°	90°
Tetragonal	90°	90°	90°
Orthorhombic	90°	180°	90°
Hexagonal	90°	60°	180°
Trigonal	90°	120°	360°
Monoclinic	90°	360°	180°
Triclinic	180°	360°	360°

It should be mentioned here that the present grain boundary identification scheme can be extended to non-cubic crystalline materials. The only difference is that the Euler space should be extended as listed in Table 1. Further, the scheme for grain boundary identification and grain boundary energy calculation can be equally applied to interfaces between different phase grains.

In summary, a scheme to identify individual grain boundaries among an infinite number of possible grain boundaries in polycrystalline materials is now available. The derivatives of the grain boundary energy with respect to inclination angles, necessary for grain growth simulations by phase-field modeling, can be easily obtained using the scheme, which allows us to construct a grain boundary energy database in a suitable form for implementation on mesoscale simulation codes for prediction of microstructure evolution based on realistic crystallographic grain orientations. The scheme can be equally applied to identify grain boundaries in face-centered cubic (fcc) materials and also to identify fcc/bcc interfaces, for example, and enables a simulation of phase transformations as well as grain growth, assigning real crystallographic orientations to individual grains.

[1] K.G.F. Janssens, D.L. Olmsted, E.A. Holm, S.M. Foiles, S.J. Plimpton, P.M. Derlet, Nat. Mater. 5 (2006) 124.
[2] D.L. Olmsted, S.M. Foiles, E.A. Holm, Acta Mater. 57 (2009) 3694.
[3] D.L. Olmsted, S.M. Foiles, E.A. Holm, Acta Mater. 57 (2009) 3704.
[4] B.-J. Lee, S.-H. Choi, Modell. Simul. Mater. Sci. Eng. 12 (2004) 621.
[5] G.J. Wang, A.P. Sutton, V. Vitek, Acta Metall. 32 (1984) 1093.
[6] G.J. Wang, V. Vitek, Acta Metall. 34 (1986) 951.
[7] A.P. Sutton, R.W. Balluffi, Acta Metall. 35 (1987) 2177.
[8] D. Schwartz, P.D. Bristowe, V. Vitek, Acta Metall. 36 (1988) 675.
[9] D. Wolf, Acta Metall. 37 (1989) 1983.
[10] D. Wolf, Acta Metall. 37 (1989) 2823.
[11] D. Wolf, Philos. Mag. B 59 (1989) 667.
[12] D. Wolf, Philos. Mag. A 62 (1990) 447.
[13] D. Wolf, Acta Metall. Mater. 38 (1990) 781.
[14] D. Wolf, Acta Metall. Mater. 38 (1990) 791.
[15] D. Wolf, J. Appl. Phys. 69 (1991) 185.
[16] M. Furtkamp, G. Gottstein, D.A. Molodov, V.N. Semenov, L.S. Shvindlerman, Acta Mater. 46 (1998) 4103.
[17] D.A. Molodov, G. Gottstein, F. Heringhaus, L.S. Shvindlerman, Acta Mater. 46 (1998) 5627.
[18] C. Schmidt, M.W. Finnis, V. Vitek, Philos. Mag. A 77 (1998) 1161.
[19] M. Upmanyu, D.J. Srolovitz, L.S. Shvindlerman, G. Gottstein, Acta Mater. 47 (1999) 3901.
[20] Y. Huang, F.J. Humphreys, Acta Mater. 48 (2000) 2017.
[21] M. Winning, G. Gottstein, L.S. Shvindlerman, Acta Mater. 50 (2002) 353.
[22] S.J. Dillon, M.P. Harmer, J. Am. Ceram. Soc. 89 (2006) 3885.
[23] D.G. Brandon, Acta Metall. 14 (1966) 1479.
[24] C. Goux, Can. Metall. Q. 13 (1974) 9.
[25] A. Morawiec, Acta Mater. 48 (2000) 3525.
[26] D.M. Saylor, A. Morawiec, G.S. Rohrer, J. Am. Ceram. Soc. 85 (2002) 3081.
[27] D.M. Saylor, A. Morawiec, G.S. Rohrer, Acta Mater. 51 (2003) 3663.
[28] D.M. Saylor, A. Morawiec, G.S. Rohrer, Acta Mater. 51 (2003) 3675.
[29] D.M. Saylor, B.S. El-Dasher, A.D. Rollett, G.S. Rohrer, Acta Mater. 52 (2004) 3649.
[30] C. Kim, Y. Hu, G.S. Rohrer, V. Randle, Scripta Mater. 52 (2005) 633.
[31] H.-J. Bunge, Texture Analysis in Materials Science, Butterworths, London, 1982.
[32] J.W. Zhao, B.L. Adams, Acta Crystallogr. Sect. A 44 (1988) 326.
[33] M.J. Wenninger, Dual Models, Cambridge University Press, Cambridge, 1983.
[34] B.-J. Lee, M.I. Baskes, Phys. Rev. B. 62 (2000) 8564.
[35] B.-J. Lee, M.I. Baskes, H. Kim, Y.K. Cho, Phys. Rev. B. 64 (2001) 184102.
[36] V. Randle, O. Engler, Introduction to Texture Analysis: Macrotexture, Microtecture and Orientation Mapping, Taylor & Francis, London, 2000.